


Hyperosmolality in CHO Culture: Effects on Proteome

Nadiya Romanova¹, Louise Schelletter¹, Raimund Hoffrogge¹ and Thomas Noll^{1*}

¹Cell culture technology, Technical Department, Bielefeld University, Bielefeld, Germany

Author Note

Nadiya Romanova nadiya.romanova@uni-bielefeld.de

Louise Schelletter  <http://orcid.org/0000-0003-2817-7919>

Raimund Hoffrogge  <https://orcid.org/0000-0003-0118-0990>

Thomas Noll  <https://orcid.org/0000-0003-0748-3423>

We have no known conflict of interest to disclose.

*Correspondence concerning this article should be addressed to Thomas Noll, Bielefeld University, Universitaetstr. 25, 33615 Bielefeld Germany. E-mail: Thomas.Noll@uni-bielefeld.de; Tel. +49 521 106-6319; Fax +49 521 106-156318

ABSTRACT

Chinese hamster ovary (CHO) is the most commonly used host cell line for therapeutic protein production. Their exposure to highly concentrated feed solution during fed-batch cultivation can cause an unphysiological osmolality increase (>300 mOsm/kg) affecting cell physiology, morphology, and proteome. In a companion article “Hyperosmolality in CHO Culture: Effects on Cellular Behavior and Morphology” we show that hyperosmolalities of up to 545 mOsm/kg force cells to ablate proliferation and gradually increase their volume, almost triplicating it. CHO cells also exhibit a significant hyperosmolality-dependent mitochondrial activity increase. To get a deeper insight into molecular mechanisms involved in these processes, we performed a comparative quantitative label-free proteome study of hyperosmolality-exposed vs. control CHO cells. Our analysis revealed key differentially expressed proteins mediating mitochondrial activation, oxidative stress amelioration, and cell cycle progression. We also discovered a previously unknown strong regulation of proteins altering cell membrane rigidity and permeability. Among others, we detected three members of septins, filamentous proteins forming diffusion barriers in the cell, to be highly upregulated in response to hyperosmolality. Taken together, our observations correlate well with the recent CHO-based fluxome and transcriptome studies and expose new unknown targets involved in response to hyperosmotic pressure in mammalian cells.

Keywords: CHO, fed-batch, hyperosmolality, cell size, LFQ proteomics

INTRODUCTION

The biopharmaceutical and biotechnological relevance of CHO cells is indisputable. Their robust growth in suspension, relative ease of genetic manipulations as well as good protein folding and post-translational modification capacity makes them the number one expression system choice for a variety of biopharmaceutical products (Sharker & Rahman, 2020).

To achieve a maximum cell density and product titer, the cells are usually cultivated in a fed-batch mode with either continuous or bolus feed addition. The used feed is a highly concentrated nutrient solution, which can cause an osmolality increase in the culture. Exposing cells to hyperosmolality leads to substantial adaptation effects, such as decreased proliferation, but also causes an unexpected cell size increase. This effect has been observed and reported previously (Kiehl et al., 2011, Pan et al., 2017, Takagi et al., 2000). In the companion article “Hyperosmolality in CHO Culture: Effects on Cellular Behavior and Morphology” we show that a step-wise increase in osmolality during fed-batch cultivation terminates cellular proliferation, and causes significant hyperosmolality-dependent mitochondrial activation and cell size increase.

Cellular response to hyperosmolality has been a focus of recent CHO-based fluxome (Pan et al., 2017) and transcriptome (Bedoya-López et al., 2016, Pan et al., 2019, Shen et al., 2010) studies. On the contrary, the last proteome investigation is dated back to 2003 (Lee et al., 2003), when two-dimensional gel electrophoresis and mass spectrometry identification delivered a total of 23 proteins, whereas only three of them had significantly different expression levels.

The technical advance of mass-spectrometry equipment, as well as CHO-specific large scale proteomic analyses (Baycin-Hizal et al., 2012, Geiger et al., 2012), changed dramatically the depth, precision, and protein identification propensity of proteome studies. In the current article, we describe results of comparative proteome analysis based on nano-scale liquid

chromatography-electrospray ionization tandem mass spectrometry (nLC-ESI-MS/MS) measurement revealing adaptation effects to hyperosmolality in CHO cells on proteome level.

1. MATERIALS AND METHODS

1.1 Experimental set-up

A detailed description of cell culture maintenance and fed-batch cultivation experiment set-up can be found in the companion article “Hyperosmolality in CHO Culture: Effects on Cellular Behavior and Morphology”. In brief, we studied the effects of high-osmolality feed exposure on suspension-adapted, antibody-producing CHO DP-12 clone#1934 (ATCC CRL-12445) cells.

For this purpose, we cultivated the cells in shaking flasks and added 6 ml of either highly supplemented, industrially relevant feed solution (“feed” condition, referred to as “F”) or supplemented medium (“control” condition, referred to as “C”) for four times on days three, four, five and six. This caused a step-wise osmolality elevation in F up to 545 mOsm/kg and no osmolality change in C. The discussion of effects on growth, cell size, and productivity as well as fed-batch growth curves are presented in the abovementioned companion article.

1.2 Proteome analysis

To analyze protein expression differences of the cells, label-free quantification mass spectrometry (LFQ-MS) was used. For LFQ-based comparison of proteomes, 1×10^7 cells of four biological replicates for each of the two conditions (feed and control) were harvested on days two, six, and eight. The cells were centrifuged at $200\times g$ for 5 min, washed in PBS once and cell pellets were stored at $-80\text{ }^{\circ}\text{C}$ until further analysis.

Cells were resuspended in 300 μl of 50 mM Tris-Buffer pH 8,0 and transferred into a new reaction tube containing approximately 150 μl of 0.1 mm glass grinding beads (Carl Roth

GmbH, Karlsruhe, Germany). All samples were processed in batch and randomized early in the workflow to minimize any possible biases. Cells were mechanically ruptured by vortexing 4x30 s and left on ice after each cycle. The supernatant was collected after 30 min centrifugation at 4 °C and 17,000×g and quantified by BCA. 20 µg of whole-cell protein were precipitated with nine parts of ice-cold acetone overnight at - 20 °C. Afterward, the samples were centrifuged for 30 min at 17,000×g, acetone was discarded and the rest was allowed to evaporate. Samples were then rehydrated in 50 mM Tris-HCl buffer, pH 8.0. Next, reduction (7 mM dithiolothreitol (DTT), 30 min, 60 °C, shaking 300 rpm), alkylation of cysteine residues (20 mM iodoacetamide (IAA), 30 min, room temperature, dark) and quenching by adding 14 mM DTT (40 min, room temperature, 300 rpm) was performed. In-solution trypsin/Lys-C (mix of Trypsin Gold and rLys-C Promega, Mannheim, Germany) digestion of 20 µg protein was performed in 1:10 dilution of 50 mM Tris-HCl buffer (pH 8.0) overnight according to manufacturer instructions (25:1 protein: protease w/w ratio). To remove any potential impurities and detergents, peptides were purified via C18 SepPak C18 vac 1cc (Waters, MA, USA) columns. In a nutshell, the column material has a strongly hydrophobic surface, able to retain even mildly hydrophobic substances. Elution was performed twice by 200 µl of 80% acetonitrile (ACN) in LC-MS grade water (Merck, Darmstadt, Germany).

1.3 nLC-ESI-MS/MS

Purified peptide mixtures of 20 µg digested whole cell lysate were resolubilized in 11 µl of LC-MS grade water with 0.1% trifluoroacetic acid (TFA) and 2,5% ACN. Using one microliter of the sample, peptide concentrations (standard deviation (sd) < 10%, absorbance at 205 nm) were measured by NanoDrop One (Thermo Fisher Scientific, Dreieich, Germany). This allowed the injection of normalized peptide amounts for the LC-MS/MS measurement. For reversed-phase peptide separation, an UltiMate 3000 RSLC nanoLC Dionex system (Thermo Fisher Scientific, Dreieich, Germany) with Acclaim PepMap™ 100 C18 pre-column cartridge

(300 μm I.D. x 5 μm , Thermo Fisher Scientific) and a 25 cm Acclaim PepMapTM 100 C18 separation column (2 μm , 75 μm I.D., Thermo Fisher Scientific, Dreieich, Germany) with an effective gradient of 1–50% solvent B (80% ACN, 1% TFA) at a flow rate of 300 nl/min within 60 min was used. Online ESI-Orbitrap mass spectrometry measurements were carried out by a Q Exactive Plus instrument (Thermo Fisher Scientific, Dreieich, Germany) in data-dependent top-10 acquisition mode, with a minimum automatic gain control (AGC) value of $1\text{e}3$ and a dynamic exclusion time of 20 seconds. Precursor ions were acquired in MS mode with a resolution of 70,000, an AGC target of $3\text{e}6$, and 80 ms maximum IT. Fragment ions were scanned with a resolution of 17,500, an AGC target of $2\text{e}5$ and an intensity threshold of 120 ms, and peptides were selected in a 1.6 mass-to-charge (m/z) isolation window for fragmentation with normalized collision energy (CE) of 28.

1.4 nLC-ESI-MS/MS data analysis

The complete LFQ-protein quantification and identification were performed in MaxQuant version 1.6.10.43 (Tyanova et al., 2016). The “matching between runs” and “LFQ” terms were selected in addition to the default parameters. Peptide quantification was performed only for the unique peptides. To enable a database search, both *Cricetulus griseus* and *Mus musculus* (UniProtKB, download on 08.07.2020, 56,327 entries for *C. griseus* and 69,504 for *M. musculus*) database were used. The following modifications were set: carbamidomethylation of cysteine (fixed modification); oxidation of methionine, N-terminal acetylation (variable modifications). The maximum number of missed cleavages was set to two and a false discovery rate (FDR) of 0.01 was selected for protein and peptide identification. The resulting data was subsequently processed in Perseus version 1.6.14.0 (Tyanova et al., 2016).

The evaluation workflow was set according to guidelines published by Tyanova *et al* (Tyanova & Cox, 2018). It covers the following steps: excluding in “proteingroups.txt” proteins only identified by site, potential contaminants, and those matching reverse database. The intensities were log2 transformed and filtered for valid values (found in at least three samples). The entries were complemented by gene annotations from Gene Ontology cellular component (GOCC), Reactome, gene set enrichment analysis (GSEA), Kyoto encyclopedia of genes and genomes (KEGG) (Kanehisa et al., 2016), CORUM molecular complexes database (Ruepp et al., 2007), mouse genome identifier (MGI), evolutionary genealogy of genes: Non-supervised Orthologous Groups (eggNOG) (Huerta-Cepas et al., 2018), SMART/PFAM (Letunic & Bork, 2017) and InterPro (Finn et al., 2016).

Categorical column annotation included three sampling points (day two, day six, and day eight), whereas each group included four biological replicates for each condition (feed and control). Categorical columns were subjected to a two-sided two-sample *t*-test, which determines if the mean LFQ-intensity values of two samples or groups are significantly different from each other, assuming their normal distribution. For the two-sample *t*-test, permutation-based FDR was set to < 0.05 , the probability value $p < 0.02$ was considered significant and S0 was set to 0. To visualize the differentially expressed proteins between control and feed conditions on days six and eight, hierarchical clustering as a heat map was used. After applying the two-sample *t*-tests (“feed” vs. “control” on day six and day eight) we used a Fisher exact test to find significantly enriched terms in gene annotations of differentially expressed genes. All graphics represented here were exported directly from the Perseus environment.

The STRING (Search Tool for the Retrieval of Interacting Genes/Proteins) was used for critical assessment and integration of protein-protein interactions (<http://string-db.org/>). The interactions are drawn both from direct experimental evidence and are predicted based on

similarities known for other organisms (Chan, 2006). By using STRING, the 41 proteins resulting from Fisher exact test based on significantly regulated proteins between “feed” and “control” for day eight (except for nidogen 1.2, as only one isoform is listed in the database) earlier were mapped and a network image was created (Figure 2).

2. RESULTS AND DISCUSSION

To elucidate the differences in protein expression between the CHO cells exposed to high-osmolality feed and those cultivated under normal conditions, we conducted a LFQ-MS experiment of the CHO DP-12 proteomes. We also intended to get a more detailed insight into mitochondrial regulation in response to osmotic pressure observed via flow cytometry and presented in the results in the companion article “Hyperosmolality in CHO Culture: Effects on Cellular Behavior and Morphology”.

The samples for LFQ-MS were harvested from four biological replicates at three points in time: day two (beginning of the exponential phase, reference point for both control and feed conditions), day six (exponential phase), and day eight (stationary phase, the onset of glucose-limitation in control). After sample preparation and tryptic digest, measurements were performed in a randomized order in one batch of nanoLC-ESI-MS acquisitions. The MS data evaluation was run on the MaxQuant version 1.6.10.43 software (Tyanova et al., 2015). The resulting “protein groups” data was loaded into the Perseus environment (version 1.6.14.0) (Tyanova et al., 2016) for statistical evaluation. Based on LFQ-MS, a total of 2881 proteins (without filtering) were identified for CHO-DP12 cells in our set-up. After filtering for those occurring in at least three samples, a total of 1771 proteins were quantified (Figure 1, a). The data delivered similar coverage compared to other recent LFQ-MS CHO proteome studies (Kaushik et al., 2020, Schelleter et al., 2019). A complete list of the identified proteins is available in electronic supply materials (Proteome Data SuppInfo, Excel-Table “All Identified

Proteins”). The biological replicates were grouped categorically for further processing. Two-sample *t*-tests with permutation-based FDR <0.05 between day six “feed” vs. “control” and day eight “feed” vs. “control” groups were run to explicate the proteins with a significantly altered expression between these two cultivation conditions. The output inherited 182 statistically significant hits between “feed” and “control” on day eight and 176 hits for day six (Figure 1, a). The complete lists of these proteins with corresponding log₂ fold changes between tested groups (“feed” vs. “control”, day six and day eight) are deposited in supplementary materials (Proteome Data SuppInfo, Excel-Table “LFQ Int. T-Test D8 D6”).

The differentially expressed proteins resulting from the categorical *t*-tests between control and feed condition on days six and eight are illustrated in Figure 1, panels b-d. Profile plots of the log₂-ratios for “feed” vs. “control” (panel b) are based on the hierarchical clustering map in panel c. They show two distinctly regulated clusters: 86 proteins were significantly up- and 96 down-regulated in the feed compared to the control condition (day eight). On the volcano plots (Figure 1, d) differentially expressed proteins are represented as a function of difference and statistical significance (*t*-test fold change vs. $-\log_{10} p$ -value). For the vast majority of the proteins, the regulation had the same trend on both days six and eight: an up-regulated protein in “feed” on day six was also up-regulated on day eight and vice versa. Out of 182 proteins with altered regulation reaching the *t*-test significance threshold (permutation-based FDR<0.05) on day eight, 88 were also deemed significant on day six.

Enriched annotations of regulated proteins on day eight reveal mitochondrial metabolism activation, basement membrane alterations, and response to oxidative stress

The discovered differentially expressed proteins between “feed” and “control” were subjected to Fischer exact test with Benjamini–Hochberg false discovery rate (BH-FDR) <0.02. The test allowed to detect enriched molecular signature terms throughout Gene Ontology cellular component (GOCC), Reactome, gene set enrichment analysis (GSEA), Kyoto encyclopedia of

genes and genomes (KEGG), and the CORUM molecular complexes database gene sets. The significant annotations had an adjusted p -value < 0.05 (after Benjamini–Hochberg false rate discovery correction). The initial Fisher exact test clustering can be found in supplementary materials ((Proteome Data SuppInfo Excel-Table “Fisher Exact D8 B-H 0.02” and Fisher Exact D6 B-H 0.02).

For day eight, three distinct major annotations containing a total of 42 non-duplicated genes were found: “extracellular matrix” (GO:0031012), “mitochondrial part” (GO:044429), and the term “GSE11057_NAIVE_VS_CENT_MEMORY_CD4_TCELL_UP” comprising genes involved in metabolic processes, stress response, and cell cycle progression. Proteins categorized in more than one cluster were manually assigned to the set with a higher enrichment factor and a lower p -value. The resulting proteins were manually curated and annotated with their main biological function based on sequence homology and biological functions described in the scientific literature. The resulting clusters are represented in Table 1. By using STRING, these 41 proteins (only one isoform, nidogen 1.1, was used) containing enriched annotation terms were mapped and a network image was created to highlight the interconnectivity between the proteins (Figure 2). STRING visualizes interactions based either on similarity or existing evidence and can be used as an additional tool to get an overview of protein scape alterations between samples.

As expected, STRING linked the members of citrate cycle Mdh2, Cs, PDH-A1, and DLD with the highest confidence scores (Figure 2), but also the members of the extracellular matrix cluster were mostly interconnected within STRING (circled in light blue).

The “extracellular matrix” cluster encompasses the abundant membrane proteins App (amyloid-beta A4 protein), Sparc (kazal-like domain-containing protein) and Lama5 (laminin) and mostly secreted proteins such as Nid1.1 and Nid 1.2 (nidogen) and Col6a1 (collagen, also in the top-10 list) and Tinagl1 (tubulointerstitial nephritis antigen-like, also in the top-10 list).

All of these proteins were less abundant on day eight in feed *versus* control condition. This may be attributed to cells' striving to redirect energy to support more vital processes and cut back on energetically expensive, but vitally inferior secretome. To support this idea, recent research has shown that nitrogen and Tinagl knock-out mutants were not hampered in cell growth and achieve even higher VCDs compared to the wild type (WT) (Kol et al., 2020).

The cluster "genes involved in stress response" (Table 1) includes protein chaperones, peroxidases, and proteasome subunits active in protein degradation. Activation of oxidative stress response upon exposure to osmotic pressure has been reported for other cells (Li, Liu, Zeng & Wei, 2017, Xu et al., 2019), and for CHO cells (Pan et al., 2019). Likely, that increase of numerous proteins involved in ROS sequestration in the cells exposed to high osmolality feed is a response to the activation of oxidative metabolism in mitochondria and not vice versa.

Significant enrichment of proteins involved in mitochondrial regulation and function (Cluster IV in Table 1) provides strong evidence in support of our findings concerning mitochondrial activity based on flow cytometry fluorescence measurements (please refer to the companion article "Hyperosmolality in CHO Culture: Effects on Cellular Behavior and Morphology"). In a pioneering proteome study of CHO under osmotic stress, the two identified up-regulated proteins pyruvate kinase and glyceraldehyde-3-phosphate dehydrogenase were related to mitochondrial oxidative metabolism (Lee et al., 2003). All genes belonging to this cluster are up-regulated in the feed condition. The mitochondrial elongation factor Tu (*Tufm*) participates in mitochondria replication, many others reflect how exactly the mitochondrial metabolic activity is regulated. The proteins coded by genes *Hadha*, *Hsd17b10*, *Cpt2*, *Hmgcl* regulate beta fatty acid oxidation and participate in lipid metabolism. Recent findings elucidate the clear connection between mitochondrial fatty acids metabolism, lipid droplets formation (previously reported for CHO under increased osmolality conditions (Pan et al., 2017)) and cellular stress response (Jarc & Petan, 2019).

Lipid droplets help to maintain membrane saturation and prevent peroxidation damage (Ackerman et al., 2018). They serve as an energy storage buffer, supplying lipids for energy production thus enabling the survival of the stressed cells. Fatty acid oxidation in mitochondria increases NADPH levels in stressed cells (Jeon et al., 2012), which is in turn consumed for the regeneration of reduced glutathione (GSH), serving as a substrate for glutathione peroxidase (Gpx4, included in cluster II (log2 fold change F vs. C D8 +1,04) and Gpx1 (log2 fold change F vs. C D8 +3,56) in the top-10 list) to eliminate H₂O₂.

Thus, proteomic results prove the interconnection between the lipid droplets accumulation and a significant increase in mitochondrial fatty acid oxidation activity.

Table 1 Genes with significantly enriched molecular annotations based on differentially expressed proteins (p < 0.01, BH-FDR < 0.02) between feed and control conditions found on proteome level during the fed-batch cultivation of CHO DP-12 cells on day eight. The letter (m) stands for “mitochondrial”.

Gene Name	Protein Name	UniProt AC	Mean log2 fold change	Biological function
I. Genes in connection with extracellular matrix/membrane				
1 <i>Col6a1</i>	Collagen alpha-1(VI) chain	G3H8Y5	-2.82	Part of extracellular matrix
2 <i>Lama5</i>	Laminin subunit alpha-5	G3HGW6	-1.57	Integrin binding, basement membrane
3 <i>Tinagl1</i>	Tubulointerstitial nephritis antigen-like	G3H1W4	-2.64	Laminin binding, cys-type peptidase
4 <i>I79_018113</i>	Nidogen 1.1	G3I3U5	-1.13	Basement membrane protein
5 <i>I79_015301</i>	Nidogen 1.2	G3HWE4	-0.91	Cell matrix adhesion
6 <i>Hspg2</i>	Heparan sulfate core protein (preliminary)	A0A3L7I8L8	-1.99	Basement membrane protein
7 <i>Sparc</i>	Kazal-like domain-containing protein	G3H584	-1.69	Collagen binding, calcium ion binding
8 <i>App</i>	Amyloid-beta A4 protein	G3HMG4	-1.88	Integral membrane component
II. Genes involved in stress response				
1 <i>Hsp90b1</i>	HSP90, beta	Q91V38	0.71	Unfolded protein binding
2 <i>Gpx4</i>	Glutathione peroxidase-4	G3HF60	1.04	Glutathione peroxidase activity
3 <i>Clu</i>	Clusterin	G3HNI3	0.80	Protein folding chaperone
4 <i>Hsph1</i>	Heat shock 105 kDa protein	G3GWF4	0.51	Prevents protein aggregation
5 <i>Psmb5</i>	Proteasome subunit beta type-5	G3HRD9	0.77	Response to oxidative stress
6 <i>Hspa9</i>	Stress-70 protein, mitochondrial	G3HEZ0	0.83	Unfolded protein binding
7 <i>Pxdn</i>	Peroxidasin-like protein	G3HBI1	-0.67	Response to oxidative stress
8 <i>Ciapi1</i>	Anamorsin	G3HIL4	-0.91	Anti-apoptotic effector
9 <i>Anxa1</i>	Annexin A1	G3I5L3	-0.72	Inflammatory response
10 <i>Glg1</i>	Golgi apparatus protein 1	G3I369	-1.95	Neg. regulation of protein processing
III. Genes involved in mitochondrial regulation and function				
1 <i>Acadvl</i>	VLC-specific acyl-CoA dehydrogenase (m)	G3GYA2	1.19	Fatty acids β -oxidation
2 <i>Ethe1</i>	Persulfide dioxygenase ETHE1 (m)	A0A061HTS8	1.01	Suppress p53-induced apoptosis
3 <i>Hmgcl</i>	Hydroxymethylglutaryl-CoA lyase (m)	G3HNV6	0.77	Lipid metabolic process
4 <i>Mdh2</i>	Malate dehydrogenase (m)	G3HA23	0.89	Carbohydrate metabolic activity
5 <i>Grpel1</i>	GrpE protein homolog 1 (m)	G3GWC4	0.98	Protein folding, mitochondrial import
6 <i>Hadha</i>	Trifunctional enzyme subunit alpha (m)	G3GXQ3	0.79	Fatty acids β -oxidation
7 <i>Hsd17b10</i>	3-hydroxyacyl-CoA dehydrogenase	G3H7U0	0.74	Fatty acids β -oxidation
8 <i>Pdha1</i>	Pyruvate dehydrogenase E1, subunit α	G3H5K6	0.88	Pyruvate oxidation
9 <i>Fdxr</i>	NADPH:adrenodoxin oxidoreductase (m)	G3GTG7	0.52	Cholesterol metabolism
10 <i>Ivd</i>	Isovaleryl-CoA dehydrogenase (m)	G3ICJ8	1.18	Leucine catabolism
11 <i>Dld</i>	Dihydrolipoyl dehydrogenase (m)	G3H8L2	0.94	Mitochondrial e- transport
12 <i>Cpt2</i>	Carnitine O-palmitoyltransferase 2 (m)	G3GTN3	0.62	Fatty acid metabolism
13 <i>Hagh</i>	Hydroxyacylglutathione hydrolase (m)	G3HBP3	0.98	Glutathione metabolism
14 <i>Shmt2</i>	Serine hydroxymethyltransferase (m)	G3HW36	0.65	Tetrahydrofolate interconversion
15 <i>Ssbp1</i>	Single-stranded DNA-binding protein (m)	G3HGL0	1.51	Mitochondrial DNA replication
16 <i>Cs</i>	Citrate synthase (m)	G3HRP3	0.82	Oxidative metabolism, TCA cycle
17 <i>Sdhaf2</i>	Succinate dehydrogenase assembly f.2 (m)	G3IER1	0.46	Chaperone
18 <i>Tufm</i>	Elongation factor Tu (m)	G3GX09	0.90	Mitochondrial elongation translation
IV. Genes involved in cell cycle progression				
1 <i>Snx9</i>	Sorting nexin-9	G3HFW9	-0.82	Mitotic cytokinesis
2 <i>Ddx3x</i>	ATP-dependent RNA helicase	G3GSH5	-0.62	Promotes G1/S-phase cell cycle transition
3 <i>Stat3</i>	Signal transducer and activator of transcripti	G3HLW9	-1.49	Regulation of cell cycle and transcription
V. Non-mitochondrial metabolic processes				
1 <i>Nucb2</i>	Nucleobindin	G3IF52	0.59	Calcium level maintenance
2 <i>Eea1</i>	Early endosome antigen	G3I600	-0.42	Endosomal trafficking
3 <i>Phgdh</i>	D-3-phosphoglycerate dehydrogenase	G3HP75	-0.98	L-serine biosynthesis

The cluster of proteins associated with cell cycle progression comprising three proteins down-regulated in feed correlates with cell cycle arrest observed by flow cytometry measurements.

The Ddx3x protein specifically promotes G₁/S-phase transition and is down-regulated in the feed condition (log₂ fold change F vs. C D8 -0,62) on day eight.

The last cluster contains three gens involved in calcium-level maintenance (nucleobindin, an abundant Golgi-protein with high affinity to Ca²⁺ (Lin et al., 1999), log₂ fold change F vs. C D8 +0,59) and proteins involved in endosomal trafficking and L-serine biosynthesis. Ca²⁺ is a by-product of mitochondrial oxidative respiration and, in higher concentrations, is toxic to the cell (Zorov et al., 2014). Nucleobindin binds and stores excessive calcium protecting cells from its damaging effects. Thus, its increased abundance in “feed” cells is likely to be connected to the increased mitochondrial activity, found both on proteome level and via flow cytometry (depicted in the companion article “Hyperosmolality in CHO Culture: Effects on Cellular Behavior and Morphology”).

The top-10 up-regulated proteins counteract oxidative stress, mediate cell cycle arrest, and increase membrane stability

We evaluated the top-10 up- and down-regulated proteins between “feed” and “control” on day six and eight (Table 2).

In Table 2, the first part is dedicated to the top-10 hits shared by both time-points followed by exclusive proteins for day eight and day six. Mean log₂ fold changes were calculated for intensities in “feed” vs. “control” groups. Positive numbers indicate the up- and negative numbers the down-regulation in feed on the indicated time point, respectively. The proteins in the top-10 list are marked with “++”, the proteins which are not in the top-10 list but are still significantly regulated (permutation-based FDR < 0.05) are marked with “+”.

Among the top-10 up-regulated proteins in “feed”, six were shared between days six and eight. The two top hits, cornifin A and high mobility group proteins A1 (HMGA1, formerly HMG-

I/HMG-Y) are involved in cell cycle progression (Tesfaigzi et al., 2003) and mitogen-activated protein kinases (MAPKs)-mediated stress response (Schuldenfrei et al., 2011).

Cornifin A (\log_2 fold change F vs. C D8 +4.92, D6 +3.91) belongs to the small proline-rich proteins (SPRR) family, which is expressed in CHO cells and is related to peptide cross-linking. Cornifin A becomes cross-linked with membrane proteins and thus might influence cell-envelope permeability (Marvin et al., 1992). It has been quantified in all biological replicates both in “feed” and in “control”. Its homolog has also been identified in non-differentiating CHO cells (Tesfaigzi & Carlson, 1996). The hallmark of the SPRR gene family is the tandem repeat of either eight (SPRR1 and SPRR3) or nine (SPRR2) amino acids with the general consensus XKXPEPXX where X is any amino acid, highly conserved between species (Gibbs et al., 1993).

The first indication of SPRR1 relation to cell cycle arrest in CHO cells dates back to 1996 (Tesfaigzi & Carlson, 1996). The same authors linked an increased expression of SPRR1B, a paralog of SPRR1A, to cells’ withdrawal from proliferative state and disruption of normal mitosis (Tesfaigzi et al., 2003). The up-regulation of SPRR1 in “feed” on both sampling points delivers a possible unexpected connection to the proliferation deregulation in CHO exposed to osmolality increase and also its role in membrane permeability regulation.

Table 2 The top-10 significantly regulated proteins on day six (D6) and eight (D8) between feed and control conditions during the fed-batch cultivation of CHO DP-12 cells. The proteins in the top-10 list are marked with “++” for D6 or D8, the proteins not in the top-10 list but still significantly regulated (permutation-based FDR < 0.05) on D6 or D8 are marked with “+”.

Gene Name	Protein Name	UniProt AC	Log2 fold change F/C		Top-10		Biological Function
			D8	D6	D8	D6	
Top-10 Up-regulated day 8 and day 6							
1 <i>Sprr1a</i>	Cornifin A	G3IIK9	4.92	3.91	++	++	Mitosis disruption
2 <i>Hmga1</i>	High mobility group A1 proteins	G3IC63	3.65	3.19	++	++	Down-reg. cell proliferation
3 <i>Gpx1</i>	Glutathione peroxidase 1 (m)	G3H8G0	3.57	0.70	++	+	Cellular stress response
4 <i>I79_001876</i>	Ribosome-binding protein 1	G3GVX1	3.16	3.77	++	++	UPR in ER
5 <i>Nono</i>	Nono protein	A0A3L7H5A3	2.81	2.87	++	++	DSB repair factor
6 <i>H671_4g12516</i>	Septin 7	G3HTJ2	2.17	2.79	++	++	Filament-forming GTPase
7 <i>Ctsz</i>	Cathepsin X	Q9EPP7	2.00	1.98	++		Carboxypeptidase
8 <i>Ranbp2</i>	E3 SUMO-protein ligase RanBP2	G3HJ15	1.95	2.16	++	++	Stress protector
9 <i>Hspa5</i>	Heat Shock 70-kDa Protein 5	A0A3L7HCD3	1.73	1.04	++	+	Unfolded protein response
10 <i>Manf</i>	Mesencephalic astrocyte-derived neu	G3H8A8	1.69	1.02	++	+	Stress response
11 <i>I79_021290</i>	Septin 11	G3IC99	1.28	2.10	+	++	Filament-forming GTPase
12 <i>CgPICR_005226</i>	Annexin	A0A3L7HVV8	1.38	2.09		++	Calcium ion binding
13 <i>H671_7g18400</i>	Septin 9	G3H3G9	0.74	2.07	+	++	Filament-forming GTPase
14 <i>I79_005051</i>	Nucleolar protein 56	G3H451	0.68	1.99	+	++	Ribosome biogenesis
Top-10 Down-regulated day 8 and day 6							
1 <i>C1ra;C1rl</i>	Complement subcomponent C1r	G3GUR1	-4.33	-2.89	++	++	Ca2+ binding ser.-type protease
2 <i>Mt1</i>	Metallothionein	G3HIK0	-3.82	-3.32	++	++	Metall-ion detoxification
3 <i>Col6a1</i>	Collagen alpha-1(VI) chain	G3H8Y5	-2.82	-1.45	++	++	Part of extracellular matrix
4 <i>Tinag1l</i>	Tubulointerstitial nephritis antigen-ii	G3H1W4	-2.64	-0.93	++		Laminin binding, cys.-type peptidase
5 <i>Notch2nl</i>	Notch homolog 2 N-terminal-like (pre	A0A3L7IFL8	-2.30	-0.99	++	+	Ca2+ binding, Notch2 binding
6 <i>Nedd4</i>	E3 Ubiquitin protein ligase	A0A3L7IB07	-2.08	-1.46	++	++	Protein degradation
7 <i>Ubqln2</i>	Ubiquilin-2	G3HWU6	-2.00	-1.20	++	+	Protein degradation
8 <i>Hspg2</i>	Heparan sulfate proteoglycan core pr	A0A3L7I8L8	-1.99	0.21	++		Basement membrane proteoglycane
9 <i>Glg1</i>	Golgi apparatus protein 1	G3I369	-1.95	0.25	++		Down-reg. protein processing
10 <i>Ctla2a/Ctla2b</i>	cytotoxic T lymphocyte-associated pr	G3IGW0	-1.92	-1.49	++	++	Down-reg. protein processing
11 <i>H671_6g15591</i>	Olfactory receptor 4P4-like protein	A0A061HXS4	-0.65	-2.03		++	RNA binding factor, transmembrane
12 <i>Ftsj3</i>	pre-rRNA processing protein FTSJ3	G3HCU9	-0.51	-1.79		++	rRNA binding methyltransferase
13 <i>Pbk</i>	Lymphokine-activated killer T-cell-ori	G3HNI7	-1.40	-1.68		++	Mitotic cell cycle kinase
14 <i>Stat1</i>	Signal transducer and activator of tran	G3I9F9	n/a	-1.46		++	Centrosome doubling
15 <i>Dcps</i>	m7GpppX diphosphatase	G3HFJ1	-0.03	-1.44		++	mRNA degradation

The high mobility group A1 (HMGA1) proteins (HMGA1a and HMGA1b) (log2 fold change F vs. C D8 +3.65, D6 +3.19) are members of the high mobility group superfamily (HMG), non-histone nuclear proteins participating in numerous biological processes such as transcription, replication, cell cycle progress and apoptosis (Reeves, 2000). These proteins recognize and modify the structure of the DNA and are highly expressed in most types of malignant cells (Fusco & Fedele, 2007, Reeves & Beckerbauer, 2001).

The downstream transcriptional targets of HMGA1 are rather multifarious. Among others, they include regulation of mitogen-activated protein kinases (MAPKs) MAPK11, MAPK12, MAPK13, and MAPK14 (Schuldenfrei et al., 2011), major regulator molecules of the cell. They are rapidly activated by osmotic stress and other extracellular stress stimuli, such as UV-radiation and heat shock (for review, see (Zhou et al., 2016)). Recent research revealed

synergistic regulation of signaling dynamics between MAPK and cyclin-dependent kinases (CDKs) (Repetto et al., 2018). The significance of CDKs in cell-size increase connected to osmotic change was addressed in the most recent transcriptome study of CHO cells (Pan et al., 2019). Thus, significant up-regulation of HMGA1 proteins in CHO DP-12 cells upon exposure to high-osmolality feed accompanied by cell-size increase emphasizes the key role of their transcriptional targets, such as MAPKs, in this process.

The other top-10 up-regulated proteins include those involved in stress and unfolded protein response (corresponding genes: *Gpx1*, *Rrbp1*, *Ranbp2*, *Hspa5*, and *Manf*), DNA repair (*Nono*), and membrane stabilization (*Septin 7*, *Septin 11*, and *Septin 9*).

Mitochondrial antioxidant enzyme glutathione peroxidase-1 (Gpx1) (log2 fold change F vs. C D8 +3.57, D6 +0.69), as well as Gpx4, discussed in the previous section is an abundant mammalian selenoenzyme playing a prominent role in the cellular response to reactive oxygen species (ROS)-induced oxidative stress (Chevallier et al., 2020). The term “ROS” includes oxygen free radicals, such as superoxide anion radical ($O_2^{\cdot -}$) and hydroxyl radical ($\cdot OH$), as well as non-oxidant radicals, such as hydrogen peroxide (H_2O_2) and singlet oxygen (1O_2). Despite several antioxidant defenses, the mitochondrion appears to be the main intracellular source of these oxidants (Turrens, 2003). Gpx1 couples oxidation of glutathione, a small three-residues (γ -L-glutamyl-L-cysteinyl glycine) peptide serving as an electron donor with H_2O_2 detoxification (Espinosa-Diez et al., 2015, Ighodaro & Akinloye, 2018). Its protective role has been shown for knockout mice in coping with oxidative injury and death mediated by reactive oxygen species (Esposito et al., 2000), as well as for CHO cells exposed to oxidative stress (Aykin-Burns & Ercal, 2006).

Ribosome-binding protein 1 (RRBP1, log2 fold change F vs. C D8 +3.16, D6 +3.77) is localized on the rough endoplasmic reticulum (ER) and is part of unfolded protein response (UPR). RRBP1 is induced during cellular stress and is studied mostly in connection to different

types of cancer (Gao et al., 2016). Taken together, RRBP1 alleviates ER stress and facilitates cell survival (Tsai et al., 2013)

SUMO E3 ligase Ran-binding protein 2 (RanBP2, log₂ fold change F vs. C D8 +1.95, D6 +2.16) is a large protein with multiple functions. It is known to modulate directly responses to such deleterious stressors, as phototoxicity, infectious agents, and carcinogens (Cho et al., 2010), and also to suppress apoptosis during oxidative stress (Cho et al., 2012). Specifically, RanBP2 co-localizes with and modulates the activity of mitochondrial proteins (Patil et al., 2019). It is noteworthy that a very high up-regulation of the ortholog gene *Ranbp3l* was recently reported in a transcriptome study of the suspension-adapted CHO cells under elevated osmolality (Pan et al., 2019).

Mesencephalic astrocyte-derived neurotrophic factor (Manf, log₂ fold change F vs. C D8 +1.69, D6 +1.02), as well as Bip/Hspa5 genes, were found to be up-regulated in response to mild hypothermia in rh-tPA-producing CHO cells (Bedoya-López et al., 2016). Hspa5 is a master chaperone that assists in translocation, folding, and stabilization of nascent protein chains (Hamman et al., 1998).

An RNA- and DNA-binding non-POU domain-containing octamer-binding (NONO) protein is a candidate DNA double-strand break (DSB) repair factor, showing end-joining stimulatory activity in biochemical protein screening (Li, Shu, Li, Jaafar, Zhao & Dynan, 2017).

Septins are a family of filament-forming GTP-ases interacting with both F-actin protein and the microtubule skeleton of the cell. Three members of this family have been found in the top-10 list: septin 7 (log₂ fold change F vs. C D8 +2.17, D6 +2.79), septin 11 (log₂ fold change F vs. C D8 +1.28, D6 +2.10) and septin 9 (log₂ fold change F vs. C D8 +0.74, D6 +2.07). Their membrane-binding ability limiting the lateral diffusion of membrane proteins (Fung et al., 2014, Gilden et al., 2012) may alter the permeability and rigidity of the cellular

membrane during osmotic pressure elevation. Although there is no experimental data for CHO cells up to date, osmotic change experiments on septin-coated vesicles indeed show their increased rigidity and shape stability under hyper-osmotic conditions compared to uncoated vesicles (Beber, 2018). Finding three members of the septin family among the ten most up-regulated expression proteins in “feed” hints that increasing membrane stability and thus facilitating cellular homeostasis maintenance plays a crucial role under osmotic pressure.

Although limiting sample size to top-10 doesn’t provide a coherent picture of cellular regulation, it nonetheless gives valuable insight into predominant changes between the conditions we studied. To summarize the above, the majority of the top-10 up-regulated proteins in “feed” on day six and day eight encounter the regulatory targets involved in oxidative stress amelioration, protein aggregation mediators, and those propagating cell cycle arrest. At last, membrane properties, such as its rigidity and permeability seems to be increased via the accumulation of septins and cornifin A.

The top-10 down-regulated proteins are involved in protein degradation, RNA processing, and cell cycle arrest

Alike the up-regulation pattern on days six and eight, where six out of ten top-10 entries were common between the two time-points, half of the top-10 down-regulated proteins are shared between both time points. In Table 2, the first part is dedicated to the common hits followed by exclusive proteins for day eight and day six.

The majority of the top-10 down-regulated proteins in “feed” are involved in proteolysis (corresponding genes *C1ra/C1rl*, *Nedd4*, *Ubqln2*, *Ctla2a/Ctla2b*), and alterations in RNA processing (*H671_6g15591*, *Ftsj3*, *Dcps*). Together this might indicate that cells exposed to osmolality increase are not only engaged in protein biosynthesis as reported earlier (Pan et al., 2017), but also strive to preserve already expressed proteins from degradation. The input of

these processes would explain the accumulation of the cellular dry mass observed for CHO cells exposed to osmotic stress (Pan et al., 2017). In support of this hypothesis, it has been shown that proteasomal degradation decreases at higher oxidant levels (Breusing & Grune, 2008). It is also worth noticing that the down-regulation of proteins involved in protein degradation in the top-10 list becomes more pronounced from day six to day eight.

Besides, two of the down-regulated proteins, Ubqln2 (log2 fold change F vs. C D8 -2.00, D6 -1.20). and Nedd4 (log2 fold change F vs. C D8 -2.08, D6 -1.46) seem to be related to mitochondrial up-regulation. Ubiquilins are chaperones that protect transmembrane proteins usually exhibiting long hydrophobic regions from aggregation in the polar cytosol (Zhang et al., 2014). Ubqln1 and 2 interact specifically with mitochondrial transmembrane proteins and degrade them upon failure to be inserted into their target. To facilitate ubiquitination, ubiquilins recruit E3 ligase (coded by Nedd4) (Itakura et al., 2016). Thus, concomitant down-regulation of these two components in “feed” might indicate the cutback of mitochondrial membrane degradation. This would lead to an increase of mitochondrial fluorescence observed in feed via flow cytometry (please, refer to the companion article “Hyperosmolality in CHO Culture: Effects on Cellular Behavior and Morphology”) due to increased abundance of the membrane proteins accumulating the fluorescent dye.

Down-regulation of Pbk-coded Lymphokine-activated killer T-cell-originated protein kinase (TOPK, log2 fold change F vs. C D8 -1.40, D6 -1.68) and Stat1 (log2 fold change F vs. C D8 not quantified, D6 -1.46), coding for Signal transducer and activator of transcription (quantified only for the day eight) seem to be related to CHO cell cycle arrest observed via flow cytometry. TOPK expression maximum evolves as proliferating cells enter mitosis (Herbert et al., 2018) and its attenuation induced G1-phase cell cycle arrest in cancer cells (Zhao et al., 2020). Stat signaling is involved in numerous processes in the cell, including a

centrosome doubling during cell cycle progression in CHO cells (Metge et al., 2004) and is not required when the cells do not proliferate.

To summarize the above, the top-10 down-regulated proteins in “feed” hint towards a decrease in protein degradation, alterations in RNA processing, and are related to cells’ exit from the normal proliferative pattern.

CONCLUSIONS

Using the LFQ approach combined with subsequent statistical evaluation allowed us to elucidate the most significant proteome changes caused by exposure of CHO DP-12 cells to highly concentrated feed. In the course of this analysis, we were able to quantify a total of 1771 proteins, whereas 176 were significantly regulated on day six and 182 on day eight of the fed-batch cultivation. Specifically, we revealed significant up-regulation of the proteins mediating oxidative stress, unfolded protein response, and protein degradation. We also detected a down-regulation of multimodal regulator molecules Stat3 and Stat1 among others involved in cell cycle progression and an up-regulation of cornifin A and Ddx3x specifically mediating cell cycle arrest. Together, these regulated proteins seem to be involved in proliferation termination observed in “feed” during the fed-batch cultivation. The up-regulation of oxidative stress response proteins, members both of the top-10 list and gene ontology enrichment clusters, is likely caused by an elevated level of ROS. Mitochondria are the main source of ROS, which evolve as by-products of oxidative metabolism. Hence, higher expression of oxidative stress response proteins is likely linked to activation of mitochondrial oxidative phosphorylation and lipid oxidation, detected via molecular annotations enrichment analysis on the proteome level. Activation of both oxidative phosphorylation and lipid oxidation yield an excess of ATP, already reported in response to hyperosmolality in CHO culture (Pfizenmaier et al., 2016). The excess of energy produced by mitochondria seems to be used for the synthesis of proteins

preventing protein aggregation and alleviating oxidative stress as well as those playing a role in cellular membrane rigidity and permeability. These activated processes are accompanied by down-regulation of proteases indicating a reduction of protein degradation. Thus, continued biomass synthesis paired with protein degradation suppression and proliferation stop result in considerable cellular mass and volume accumulation.

ACKNOWLEDGMENTS

Authors would like to thank Larissa Lessmann for assistance with proteome samples preparation. This work was funded by Bielefeld University. Nadiya Romanova is supported by a Grant for women in the orientation phase initiated by the Equal Opportunities Commission of the Faculty of Technology, Bielefeld University.

CONFLICT OF INTERESTS

The authors declare that there is no conflict of interest.

AUTHOR CONTRIBUTIONS

N.R. designed and performed the experiments, carried out the sample preparation, analyzed and interpreted the data, and wrote the manuscript. L.S. conceived an initial idea of proteome analysis, contributed to the data analysis, and manuscript preparation. R.H. performed the MS/MS measurement, protocol optimization, and contributed to the manuscript preparation. T.N. conceived an initial project idea, acquired funding, and supervised the project. All authors read and approved the manuscript.

3. REFERENCES

- Ackerman, D., Tumanov, S., Qiu, B., Michalopoulou, E., Spata, M., Azzam, A., Xie, H., Simon, M. C. & Kamphorst, J. J. (2018), Triglycerides promote lipid homeostasis during hypoxic stress by balancing fatty acid saturation, *Cell reports* **24**(10), 2596–2605.e5. <https://pubmed.ncbi.nlm.nih.gov/30184495>
- Aykin-Burns, N. & Ercal, N. (2006), Effects of selenocystine on lead-exposed chinese hamster ovary (cho) and pc-12 cells, *Toxicology and Applied Pharmacology* **214**(2), 136–143. <http://www.sciencedirect.com/science/article/pii/S0041008X05006721>
- Baycin-Hizal, D., Tabb, D. L., Chaerkady, R., Chen, L., Lewis, N. E., Nagarajan, H., Sarkaria, V., Kumar, A., Wolozny, D., Colao, J., Jacobson, E., Tian, Y., OMeally, R. N., Krag, S. S., Cole, R. N., Palsson, B. O., Zhang, H. & Betenbaugh, M. (2012), Proteomic analysis of chinese hamster ovary cells., *J Proteome Res* **11**(11), 5265–5276.
- Beber, A. (2018), Invitro study of membrane remodeling and curvature sensing at the micrometric scale by budding yeast septins., tel-02015522v2, Sorbonne Université Biological Physics [physics.bio-ph]., NNT:2018SORUS375.
- Bedoya-López, A., Estrada, K., Sanchez-Flores, A., Ramrez, O. T., Altamirano, C., Segovia, L., Miranda-Rós, J., Trujillo-Roldán, M. A. & Valdez-Cruz, N. A. (2016), Effect of temperature downshift on the transcriptomic responses of chinese hamster ovary cells using recombinant human tissue plasminogen activator production culture, *PloS one* **11**(3), e0151529–e0151529. <https://pubmed.ncbi.nlm.nih.gov/26991106>
- Breusing, N. & Grune, T. (2008), Regulation of proteasome-mediated protein degradation during oxidative stress and aging, *Biological Chemistry* **389**(3), 203–209. <https://www.degruyter.com/view/journals/bchm/389/3/article-p203.xml>
- Chan, D. C. (2006), Mitochondria: dynamic organelles in disease, aging, and development., *Cell* **125**(7), 1241–1252.

Chevallier, V., Andersen, M. R. & Malphettes, L. (2020), Oxidative stress-alleviating strategies to improve recombinant protein production in cho cells, *Biotechnology and Bioengineering* **117**(4), 1172–1186. <https://doi.org/10.1002/bit.27247>

Cho, K.-i., Searle, K., Webb, M., Yi, H. & Ferreira, P. A. (2012), Ranbp2 haploinsufficiency mediates distinct cellular and biochemical phenotypes in brain and retinal dopaminergic and glia cells elicited by the parkinsonian neurotoxin, 1-methyl-4-phenyl-1,2,3,6-tetrahydropyridine (mptp), *Cellular and Molecular Life Sciences* **69**(20), 3511–3527. <https://doi.org/10.1007/s00018-012-1071-9>

Cho, K.-i., Yi, H., Tserentsoodol, N., Searle, K. & Ferreira, P. A. (2010), Neuroprotection resulting from insufficiency of ranbp2 is associated with the modulation of protein and lipid homeostasis of functionally diverse but linked pathways in response to oxidative stress, *Disease Models & Mechanisms* **3**(9-10), 595–604.

Espinosa-Diez, C., Miguel, V., Mennerich, D., Kietzmann, T., Sánchez-Pérez, P., Cadenas, S. & Lamas, S. (2015), Antioxidant responses and cellular adjustments to oxidative stress., *Redox Biol* **6**, 183–197.

Esposito, L. A., Kokoszka, J. E., Waymire, K. G., Cottrell, B., MacGregor, G. R. & Wallace, D. C. (2000), Mitochondrial oxidative stress in mice lacking the glutathione peroxidase-1 gene, *Free Radical Biology and Medicine* **28**(5), 754–766. <http://www.sciencedirect.com/science/article/pii/S0891584900001611>

Finn, R. D., Attwood, T. K., Babbitt, P. C., Bateman, A., Bork, P., Bridge, A. J., Chang, H.-Y., Dosztányi, Z., El-Gebali, S., Fraser, M., Gough, J., Haft, D., Holliday, G. L., Huang, H., Huang, X., Letunic, I., Lopez, R., Lu, S., Marchler-Bauer, A., Mi, H., Mistry, J., Natale, D. A., Necci, M., Nuka, G., Orengo, C. A., Park, Y., Pesseat, S., Piovesan, D., Potter, S. C., Rawlings, N. D., Redaschi, N., Richardson, L., Rivoire, C., Sangrador-Vegas, A., Sigrist,

- C., Sillitoe, I., Smithers, B., Squizzato, S., Sutton, G., Thanki, N., Thomas, P. D., Tosatto, S. C. E., Wu, C. H., Xenarios, I., Yeh, L.-S., Young, S.-Y. & Mitchell, A. L. (2016), Interpro in 2017—beyond protein family and domain annotations, *Nucleic Acids Research* **45**(D1), D190–D199. <https://doi.org/10.1093/nar/gkw1107>
- Fung, K. Y. Y., Dai, L., Trimble, W. S. & Jeon, K. W. (2014), *Chapter Seven - Cell and Molecular Biology of Septins*, Vol. 310, Academic Press, pp. 289–339. <http://www.sciencedirect.com/science/article/pii/B9780128001806000074>
- Fusco, A. & Fedele, M. (2007), Roles of hmga proteins in cancer, *Nature Reviews Cancer* **7**(12), 899–910. <https://doi.org/10.1038/nrc2271>
- Gao, W., Li, Q., Zhu, R. & Jin, J. (2016), La autoantigen induces ribosome binding protein 1 (rrbp1) expression through internal ribosome entry site (ires)-mediated translation during cellular stress condition, *International journal of molecular sciences* **17**(7), 1174. <https://pubmed.ncbi.nlm.nih.gov/27447629>
- Geiger, T., Wehner, A., Schaab, C., Cox, J. & Mann, M. (2012), Comparative proteomic analysis of eleven common cell lines reveals ubiquitous but varying expression of most proteins., *Mol Cell Proteomics* **11**(3), M111.014050.
- Gibbs, S., Fijneman, R., Wiegant, J., van Kessel, A. G., van De Putte, P. & Backendorf, C. (1993), Molecular characterization and evolution of the sprr family of keratinocyte differentiation markers encoding small proline-rich proteins., *Genomics* **16**(3), 630–637.
- Gilden, J. K., Peck, S., Chen, Y.-C. M. & Krummel, M. F. (2012), The septin cytoskeleton facilitates membrane retraction during motility and blebbing., *J Cell Biol* **196**(1), 103–114.
- Hamman, B. D., Hendershot, L. M. & Johnson, A. E. (1998), Bip maintains the permeability barrier of the er membrane by sealing the luminal end of the translocon pore before and early in translocation., *Cell* **92**(6), 747–758.

- Herbert, K. J., Ashton, T. M., Prevo, R., Pirovano, G. & Higgins, G. S. (2018), T-lak cell-originated protein kinase (topk): an emerging target for cancer-specific therapeutics, *Cell Death & Disease* **9**(11), 1089. <https://doi.org/10.1038/s41419-018-1131-7>
- Huerta-Cepas, J., Szklarczyk, D., Heller, D., Hernández-Plaza, A., Forslund, S. K., Cook, H., Mende, D. R., Letunic, I., Rattei, T., Jensen, L. J., von Mering, C. & Bork, P. (2018), egglog 5.0: a hierarchical, functionally and phylogenetically annotated orthology resource based on 5090 organisms and 2502 viruses, *Nucleic Acids Research* **47**(D1), D309–D314. <https://doi.org/10.1093/nar/gky1085>
- Ighodaro, O. M. & Akinloye, O. A. (2018), First line defence antioxidants-superoxide dismutase (sod), catalase (cat) and glutathione peroxidase (gpx): Their fundamental role in the entire antioxidant defence grid, *Alexandria Journal of Medicine* **54**(4), 287–293. <https://doi.org/10.1016/j.ajme.2017.09.001>
- Itakura, E., Zavodszky, E., Shao, S., Wohlever, M. L., Keenan, R. J. & Hegde, R. S. (2016), Ubiquilins chaperone and triage mitochondrial membrane proteins for degradation, *Molecular Cell* **63**(1), 21–33. <http://www.sciencedirect.com/science/article/pii/S1097276516301836>
- Jarc, E. & Petan, T. (2019), Lipid droplets and the management of cellular stress., *Yale J Biol Med* **92**(3), 435–452.
- Jeon, S.-M., Chandel, N. S. & Hay, N. (2012), Ampk regulates nadph homeostasis to promote tumour cell survival during energy stress, *Nature* **485**(7400), 661–665. <https://pubmed.ncbi.nlm.nih.gov/22660331>
- Kanehisa, M., Sato, Y., Kawashima, M., Furumichi, M. & Tanabe, M. (2016), Kegg as a reference resource for gene and protein annotation., *Nucleic Acids Res* **44**(D1), D457–62.

- Kaushik, P., Curell, R. V.-B., Henry, M., Barron, N. & Meleady, P. (2020), LC-MS/MS-based quantitative proteomic and phosphoproteomic analysis of CHO-k1 cells adapted to growth in glutamine-free media, *Biotechnology Letters* **42**(12), 2523–2536.
- Kiehl, T. R., Shen, D., Khattak, S. F., Jian Li, Z. & Sharfstein, S. T. (2011), Observations of cell size dynamics under osmotic stress, *Cytometry Part A* **79A**(7), 560–569. <https://doi.org/10.1002/cyto.a.21076>
- Kol, S., Ley, D., Wulff, T., Decker, M., Arnsdorf, J., Schoffelen, S., Hansen, A. H., Jensen, T. L., Gutierrez, J. M., Chiang, A. W. T., Masson, H. O., Palsson, B. O., Voldborg, B. G., Pedersen, L. E., Kildegaard, H. F., Lee, G. M. & Lewis, N. E. (2020), Multiplex secretome engineering enhances recombinant protein production and purity, **11**(1), 1908.
- Lee, M. S., Kim, K. W., Kim, Y. H. & Lee, G. M. (2003), Proteome analysis of antibody-expressing cho cells in response to hyperosmotic pressure, *Biotechnology Progress* **19**(6), 1734–1741. <https://doi.org/10.1021/bp034093a>
- Letunic, I. & Bork, P. (2017), 20 years of the smart protein domain annotation resource, *Nucleic Acids Research* **46**(D1), D493–D496. <https://doi.org/10.1093/nar/gkx922>
- Li, S., Shu, F.-j., Li, Z., Jaafar, L., Zhao, S. & Dynan, W. S. (2017), Cell-type specific role of the rna-binding protein, nono, in the dna double-strand break response in the mouse testes, *DNA Repair* **51**, 70–78. <http://www.sciencedirect.com/science/article/pii/S1568786416303500>
- Li, Y., Liu, H., Zeng, W. & Wei, J. (2017), Edaravone protects against hyperosmolarity-induced oxidative stress and apoptosis in primary human corneal epithelial cells., *PLoS One* **12**(3), e0174437.
- Lin, P., Yao, Y., Hofmeister, R., Tsien, R. Y. & Farquhar, M. G. (1999), Overexpression of calnuc (nucleobindin) increases agonist and thapsigargin releasable ca²⁺ storage in the

golgi, *The Journal of cell biology* **145**(2), 279–289.
<https://pubmed.ncbi.nlm.nih.gov/10209024>

Marvin, K. W., George, M. D., Fujimoto, W., Saunders, N. A., Bernacki, S. H. & Jetten, A. M. (1992), Cornifin, a cross-linked envelope precursor in keratinocytes that is down-regulated by retinoids., *Proceedings of the National Academy of Sciences* **89**(22), 11026–11030.

Metge, B., Ofori-Acquah, S., Stevens, T. & Balczon, R. (2004), Stat3 activity is required for centrosome duplication in chinese hamster ovary cells, *Journal of Biological Chemistry* **279**(40), 41801–41806.

Pan, X., Alsayyari, A. A., Dalm, C., Hageman, J. A., Wijffels, R. & Martens, D. E. (2019), Transcriptome analysis of cho cell size increase during a fed-batch process, *Biotechnology Journal* **14**(3), 1800156. <https://doi.org/10.1002/biot.201800156>

Pan, X., Dalm, C., Wijffels, R. & Martens, D. E. (2017), Metabolic characterization of a cho cell size increase phase in fed-batch cultures, *Applied microbiology and biotechnology* **101**(22), 8101–8113. <https://www.ncbi.nlm.nih.gov/pubmed/28951949>

Patil, H., Yoon, D., Bhowmick, R., Cai, Y., Cho, K.-i. & Ferreira, P. A. (2019), Impairments in age-dependent ubiquitin proteostasis and structural integrity of selective neurons by uncoupling ran gtpase from the ran-binding domain 3 of ranbp2 and identification of novel mitochondrial isoforms of ubiquitin-conjugating enzyme e2i (ubc9) and ranbp2, *Small GTPases* **10**(2), 146–161.
<https://doi.org/10.1080/21541248.2017.1356432>

Pfizenmaier, J., Junghans, L., Teleki, A. & Takors, R. (2016), Hyperosmotic stimulus study discloses benefits in atp supply and reveals mirna/mrna targets to improve recombinant protein production of cho cells., *Biotechnol J* **11**(8), 1037–1047.

Reeves, R. (2000), Structure and function of the hmgi(y) family of architectural transcription factors., *Environ Health Perspect* **108 Suppl 5**, 803–809.

Reeves, R. & Beckerbauer, L. (2001), Hmgi/y proteins: flexible regulators of transcription and chromatin structure, *Biochimica et Biophysica Acta (BBA) - Gene Structure and Expression* **1519**(1), 13–29.

<http://www.sciencedirect.com/science/article/pii/S0167478101002159>

Repetto, M. V., Winters, M. J., Bush, A., Reiter, W., Hollenstein, D. M., Ammerer, G., Pryciak, P. M. & Colman-Lerner, A. (2018), CDK and MAPK synergistically regulate signaling dynamics via a shared multi-site phosphorylation region on the scaffold protein ste5, *Molecular Cell* **69**(6), 938–952.e6.

Ruepp, A., Brauner, B., Dunger-Kaltenbach, I., Frishman, G., Montrone, C., Stransky, M., Waegelé, B., Schmidt, T., Doudieu, O. N., Stumpflen, V. & Mewes, H. W. (2007), CORUM: the comprehensive resource of mammalian protein complexes, *Nucleic Acids Research* **36**(Database), D646–D650.

Schelleter, L., Albaum, S., Walter, S., Noll, T. & Hoffrogge, R. (2019), Clonal variations in cho igf signaling investigated by silac-based phosphoproteomics and lfq-ms, *Applied Microbiology and Biotechnology* **103**(19), 8127–8143. <https://doi.org/10.1007/s00253-019-10020-z>

Schuldenfrei, A., Belton, A., Kowalski, J., Talbot, C. C., Di Cello, F., Poh, W., Tsai, H.-L., Shah, S. N., Huso, T. H., Huso, D. L. & Resar, L. M. (2011), Hmga1 drives stem cell, inflammatory pathway, and cell cycle progression genes during lymphoid tumorigenesis, *BMC Genomics* **12**(1), 549. <https://doi.org/10.1186/1471-2164-12-549>

Sharker, S. M. & Rahman, M. A. (2020), Review of the current methods of chinese hamster ovary (CHO) cells cultivation for production of therapeutic protein, *Current Drug Discovery Technologies* **17**.

Shen, D., Kiehl, T. R., Khattak, S. F., Li, Z. J., He, A., Kayne, P. S., Patel, V., Neuhaus, I. M. & Sharfstein, S. T. (2010), Transcriptomic responses to sodium chloride-induced osmotic stress: A study of industrial fed-batch CHO cell cultures, *Biotechnology Progress* pp. NA–NA.

Takagi, M., Hayashi, H. & Yoshida, T. (2000), The effect of osmolarity on metabolism and morphology in adhesion and suspension chinese hamster ovary cells producing tissue plasminogen activator, *Cytotechnology* **32**(3), 171–179.

Tesfaigzi, J. & Carlson, D. M. (1996), Cell cycle-specific expression of g0spr1 in chinese hamster ovary cells, *Experimental Cell Research* **228**(2), 277–282.
<http://www.sciencedirect.com/science/article/pii/S0014482796903274>

Tesfaigzi, Y., Wright, P. S. & Belinsky, S. A. (2003), Sprr1b overexpression enhances entry of cells into the g0 phase of the cell cycle., *Am J Physiol Lung Cell Mol Physiol* **285**(4), L889–98.

Tsai, H.-Y., Yang, Y.-F., Wu, A. T., Yang, C.-J., Liu, Y.-P., Jan, Y.-H., Lee, C.-H., Hsiao, Y.-W., Yeh, C.-T., Shen, C.-N., Lu, P.-J., Huang, M.-S. & Hsiao, M. (2013), Endoplasmic reticulum ribosome-binding protein 1 (rrbp1) overexpression is frequently found in lung cancer patients and alleviates intracellular stress-induced apoptosis through the enhancement of grp78, *Oncogene* **32**(41), 4921–4931.
<https://doi.org/10.1038/onc.2012.514>

Turrens, J. F. (2003), Mitochondrial formation of reactive oxygen species, *The Journal of Physiology* **552**(2), 335–344.

- Tyanova, S. & Cox, J. (2018), *Perseus: A Bioinformatics Platform for Integrative Analysis of Proteomics Data in Cancer Research*, Springer New York, New York, NY, pp. 133–148. https://doi.org/10.1007/978-1-4939-7493-1_7
- Tyanova, S., Temu, T., Carlson, A., Sinitcyn, P., Mann, M. & Cox, J. (2015), Visualization of LC-MS/MS proteomics data in MaxQuant, *PROTEOMICS* **15**(8), 1453–1456.
- Tyanova, S., Temu, T., Sinitcyn, P., Carlson, A., Hein, M. Y., Geiger, T., Mann, M. & Cox, J. (2016), The perseus computational platform for comprehensive analysis of (prote)omics data, *Nature Methods* **13**(9), 731–740.
- Xu, J., Li, H., Yang, K., Guo, S., Wang, J., Feng, C. & Chen, H. (2019), Hyper-osmolarity environment-induced oxidative stress injury promotes nucleus pulposus cell senescence in vitro, *Bioscience Reports* **39**(9). <https://doi.org/10.1042/BSR20191711>
- Zhang, K. Y., Yang, S., Warraich, S. T. & Blair, I. P. (2014), Ubiquitin 2: A component of the ubiquitin–proteasome system with an emerging role in neurodegeneration, *The International Journal of Biochemistry & Cell Biology* **50**, 123–126. <http://www.sciencedirect.com/science/article/pii/S1357272514000673>
- Zhao, R., Choi, B. Y., Wei, L., Fredimoses, M., Yin, F., Fu, X., Chen, H., Liu, K., Kundu, J. K., Dong, Z. & Lee, M.-H. (2020), Acetylshikonin suppressed growth of colorectal tumour tissue and cells by inhibiting the intracellular kinase, t-lymphokine-activated killer cell-originated protein kinase., *British Journal of Pharmacology* **177**(10), 2303–2319. <https://doi.org/10.1111/bph.14981>
- Zhou, X., Naguro, I., Ichijo, H. & Watanabe, K. (2016), Mitogen-activated protein kinases as key players in osmotic stress signaling., *Biochim Biophys Acta* **1860**(9), 2037–2052.
- Zorov, D. B., Juhaszova, M. & Sollott, S. J. (2014), Mitochondrial reactive oxygen species (ROS) and ROS-induced ROS release, *Physiological Reviews* **94**(3), 909–950.

4. TABLES

Table 1 Genes with significant molecular annotations based on differentially expressed proteins ($p < 0,01$) between feed and control condition found on proteome level during the fed-batch cultivation of CHO DP-12 cells on day eight. The letter (m) stands for “mitochondrial”.

Gene Name	Protein Name	UniProt AC	Mean log2 fold change D8 F/C	Biological function
I. Genes in connection with extracellular matrix/membrane				
1 <i>Col6a1</i>	Collagen alpha-1(VI) chain	G3H8Y5	-2.82	Part of extracellular matrix
		G3HGW		Integrin binding, basement membrane
2 <i>Lama5</i>	Laminin subunit alpha-5	6	-1.57	
	Tubulointerstitial nephritis antigen-like	G3H1W		Laminin binding, cys-type peptidase
3 <i>Tinagl1</i>		4	-2.64	
				Basement membrane protein
4 <i>179_01811</i>	Nidogen 1.1	G3I3U5	-1.13	
		G3HWE		
5 <i>179_01530</i>	Nidogen 1.2	4	-0.91	Cell matrix adhesion
	Heparan sulfate core protein	A0A3L7I		Basement membrane protein
6 <i>Hspg2</i>	(preliminary)	8L8	-1.99	
	Kazal-like domain-containing protein	G3H584	-1.69	Collagen binding, calcium ion binding
7 <i>Sparc</i>		G3HMG		Integral membrane component
8 <i>App</i>	Amyloid-beta A4 protein	4	-1.88	
II. Genes involved in stress response				
1 <i>Hsp90b1</i>	HSP90, beta	Q91V38	0.71	Unfolded protein binding
				Glutathione peroxidase activity
2 <i>Gpx4</i>	Glutathione peroxidase-4	G3HF60	1.04	
3 <i>Clu</i>	Clusterin	G3HNJ3	0.80	Protein folding chaperone
		G3GWF		Prevents protein aggregation
4 <i>Hsph1</i>	Heat shock 105 kDa protein	4	0.51	
	Proteasome subunit beta			
5 <i>Psmb5</i>	type-5	G3HRD9	0.77	Response to oxidative stress
	Stress-70 protein,			
6 <i>Hspa9</i>	mitochondrial	G3HEZ0	0.83	Unfolded protein binding
7 <i>Pxdn</i>	Peroxidasin-like protein	G3HBI1	-0.67	Response to oxidative stress
8 <i>Ciapi1</i>	Anamorsin	G3HIL4	-0.91	Anti-apoptotic effector
9 <i>Anxa1</i>	Annexin A1	G3I5L3	-0.72	Inflammatory response
				Neg. regulation of protein processing
10 <i>Glg1</i>	Golgi apparatus protein 1	G3I369	-1.95	
III. Genes involved in mitochondrial regulation and function				
1 <i>Acadvl</i>	VLC-specific acyl-CoA dehydrogenase (m)	G3GYA2	1.19	Fatty acids β -oxidation

2	<i>Ethe1</i>	Persulfide dioxygenase ETHE1 (m)	A0A061 HTS8	1.01	Suppress p53-induced apoptosis
3	<i>Hmgcl</i>	Hydroxymethylglutaryl-CoA lyase (m)	G3HMV 6	0.77	Lipid metabolic process Carbohydrate metabolic activity
4	<i>Mdh2</i>	Malate dehydrogenase (m)	G3HA23 G3GWC	0.89	Protein folding, mitochondrial import
5	<i>Grpel1</i>	GrpE protein homolog 1 (m) Trifunctional enzyme	4	0.98	
6	<i>Hadha</i>	subunit alpha (m) 3-hydroxyacyl-CoA	G3GXQ3	0.79	Fatty acids β -oxidation
7	<i>Hsd17b10</i>	dehydrogenase Pyruvate dehydrogenase E1,	G3H7U0	0.74	Fatty acids β -oxidation
8	<i>Pdha1</i>	subunit α NADPH:adrenodoxin	G3H5K6	0.88	Pyruvate oxidation
9	<i>Fdxr</i>	oxidoreductase (m) Isovaleryl-CoA	G3GTG7	0.52	Cholesterol metabolism
10	<i>Ivd</i>	dehydrogenase (m) Dihydrolipoyl	G3ICJ8	1.18	Leucine catabolism
11	<i>Dld</i>	dehydrogenase (m) Carnitine O-	G3H8L2	0.94	Mitochondrial e- transport
12	<i>Cpt2</i>	palmitoyltransferase 2 (m) Hydroxyacylglutathione	G3GTN3	0.62	Fatty acid metabolism
13	<i>Hagh</i>	hydrolase (m) Serine	G3HBP3	0.98	Glutathione metabolism
14	<i>Shmt2</i>	hydroxymethyltransferase (m)	G3HW3 6	0.65	Tetrahydrofolate interconversion
15	<i>Ssbp1</i>	Single-stranded DNA- binding protein (m)	G3HGL0	1.51	Mitochondrial DNA replication
16	<i>Cs</i>	Citrate synthase (m) Succinate dehydrogenase	G3HRP3	0.82	Oxidative metabolism, TCA cycle
17	<i>Sdhaf2</i>	assembly f.2 (m)	G3IER1	0.46	Chaperone
18	<i>Tufm</i>	Elongation factor Tu (m)	G3GX09	0.90	Mitochondrial elongation translation

IV. Genes involved in cell cycle progression

1	<i>Snx9</i>	Sorting nexin-9 ATP-dependent RNA	G3HFW 9	-0.82	Mitotic cytokinesis Promotes G1/S-phase cell cycle transition
2	<i>Ddx3x</i>	helicase	G3GSH5	-0.62	Regulation of cell cycle and transcription
3	<i>Stat3</i>	Signal transducer and activator of transcription 3	G3HLW 9	-1.49	

V. Non-mitochondrial metabolic processes

1	<i>Nucb2</i>	Nucleobindin	G3IF52	0.59	Calcium level maintenance
2	<i>Eea1</i>	Early endosome antigen D-3-phosphoglycerate	G3I600	-0.42	Endosomal trafficking
3	<i>Phgdh</i>	dehydrogenase	G3HP75	-0.98	L-serine biosynthesis

Table 2. The top-10 significantly regulated proteins on day six (D6) and eight (D8) between feed and control conditions during the fed-batch cultivation of CHO DP-12 cells. The proteins in the top-10 list are marked with “++” for D6 or D8, the proteins not in the top-10 list but still significantly regulated (permutation-based FDR < 0.05) on D6 or D8 are marked with “+”.

Gene Name	Protein Name	UniProt AC	Log2 fold change F/C		Top-10		Biological Function
			D8	D6	D8	D6	
Top-10 Up-regulated day 8 and day 6							
1 <i>Sprr1a</i>	Cornifin A	G3IIK9	4.92	3.91	++	++	Mitosis disruption
2 <i>Hmga1</i>	High mobility group A1 proteins	G3IC63	3.65	3.19	++	++	Down-reg. cell proliferation
3 <i>Gpx1</i>	Glutathione peroxidase 1 (m)	G3H8G0	3.57	0.70	++	+	Cellular stress response
4 <i>I79_001876</i>	Ribosome-binding protein 1	G3GVX1	3.16	3.77	++	++	UPR in ER
5 <i>Nono</i>	Nono protein	A0A3L7H5A3	2.81	2.87	++	++	DSB repair factor
6 <i>H671_4g12516</i>	Septin 7	G3HTJ2	2.17	2.79	++	++	Filament-forming GTPase
7 <i>Ctsz</i>	Cathepsin X	Q9EPP7	2.00	1.98	++		Carboxypeptidase
8 <i>Ranbp2</i>	E3 SUMO-protein ligase RanBP2	G3HJ15	1.95	2.16	++	++	Stress protector
9 <i>Hspa5</i>	Heat Shock 70-kDa Protein 5	A0A3L7HCD3	1.73	1.04	++	+	Unfolded protein response
10 <i>Manf</i>	Mesencephalic astrocyte-derived neurotrophic factor	G3H8A8	1.69	1.02	++	+	Stress response
11 <i>I79_021290</i>	Septin 11	G3IC99	1.28	2.10	+	++	Filament-forming GTPase
12 <i>CgPICR_005226</i>	Annexin	A0A3L7HVV8	1.38	2.09		++	Calcium ion binding
13 <i>H671_7g18400</i>	Septin 9	G3H3G9	0.74	2.07	+	++	Filament-forming GTPase
14 <i>I79_005051</i>	Nucleolar protein 56	G3H451	0.68	1.99	+	++	Ribosome biogenesis
Top-10 Down-regulated day 8 and day 6							
1 <i>C1ra;C1rl</i>	Complement subcomponent C1r	G3GUR1	-	4.33	-2.89	++	Ca2+ binding ser.-type protease
2 <i>Mt1</i>	Metallothionein	G3HIK0	-	3.82	-3.32	++	Metal-ion detoxification
3 <i>Col6a1</i>	Collagen alpha-1(VI) chain	G3H8Y5	-	2.82	-1.45	++	Part of extracellular matrix
4 <i>Tinagl1</i>	Tubulointerstitial nephritis antigen-like	G3H1W4	-	2.64	-0.93	++	Laminin binding, cys.-type peptidase

5	<i>Notch2nl</i>	Notch homolog 2 N-terminal-like (preliminary data)	A0A3L7IFL8	2.30	-0.99	++	+	Ca ²⁺ binding, Notch2 binding
6	<i>Nedd4</i>	E3 Ubiquitin protein ligase	A0A3L7IB07	2.08	-1.46	++	++	Protein degradation
7	<i>Ubqln2</i>	Ubiquilin-2	G3HWU6	2.00	-1.20	++	+	Protein degradation
8	<i>Hspg2</i>	Heparan sulfate proteoglycan core protein (preliminary)	A0A3L7I8L8	1.99	0.21	++		Basement membrane proteoglycane
9	<i>Glg1</i>	Golgi apparatus protein 1	G3I369	1.95	0.25	++		Down-reg. protein processing
10	<i>Ctla2a/Ctla2b</i>	cytotoxic T lymphocyte-associated protein 2 alpha/beta	G3IGW0	1.92	-1.49	++	++	Down-reg. protein processing
11	<i>H671_6g15591</i>	Olfactory receptor 4P4-like protein	A0A061HXS4	0.65	-2.03		++	RNA binding factor, transmembrane
12	<i>Ftsj3</i>	pre-rRNA processing protein FTSJ3	G3HCU9	0.51	-1.79		++	rRNA binding methyltransferase
13	<i>Pbk</i>	Lymphokine-activated killer T-cell-originated protein kinase	G3HNI7	1.40	-1.68		++	Mitotic cell cycle kinase
14	<i>Stat1</i>	Signal transducer and activator of transcription	G3I9F9	n/a	-1.46		++	Centrosome doubling
15	<i>Dcps</i>	m7GpppX diphosphatase	G3HFJ1	0.03	-1.44		++	mRNA degradation

5. FIGURE LEGENDS

Figure 1

Proteome analysis data across three cultivation time points for the fed-batch cultivation of CHO DP-12 cells exposed to high osmolality (“feed”, F) or without osmotic change (“control”, C). a) Numbers of quantified and significantly regulated (permutation-based FDR 0.05) proteins between F and C found in CHO proteomes; b) Profile plots of the log₂-ratios F vs. C of the two clusters based on heatmap c); cluster 1 – proteins with significantly decreased expression on day six and eight in the feed condition; 2 – proteins with a significantly increased expression on day six and eight in the feed condition. c) Hierarchical clustering of significantly regulated proteins across three cultivation time points for the fed-batch cultivation of CHO DP-12 cells. High and low expression is shown in red and green respectively (“T” is an abbreviation for “day” (Tag), “C” indicates control, and “F” feed condition. Number after the letter indicates biological replicate). d) Volcano plots of average abundances in four biological replicates for significantly regulated proteins on day six and day eight in F and C. The

plot is represented as a function of statistical significance (t-test $p \leq 0.1$ and fold change cut-off point ± 0) between control and feed condition isolates. The Y-axis indicates p-value ($-\log_{10}$). The X-axis shows the protein ratio (\log_2 change) in C vs. F conditions. Proteins significantly up-regulated in the feed are highlighted with pink ovals, proteins significantly down-regulated with light blue ones. The top-10 proteins (up-regulated in feed) are marked with red dots; the top-10 proteins down-regulated in feed –blue dots. Proteins with no statistically significant expression differences between the two conditions are shown in grey under the significance cut-off curve.

Figure 2

STRING visualization of the significantly regulated proteins with enriched annotations resulting from Fischer exact test BH-FDR < 0.02 listed in Table 1. The nodes are the proteins and the connecting lines represent STRING interaction (according to STRING: red line - fusion evidence; green line - neighborhood evidence; blue line – co-occurrence evidence; purple line - experimental evidence; yellow line - textmining evidence; light blue line - database evidence; black line – co-expression evidence). Proteins of the extracellular cluster are circled in light blue. The table below represents confidence scores (the approximate probability that a predicted link exists in the same KEGG metabolic map) of the interaction nodes. A confidence score of ≥ 0.7 means “high confidence” and of ≥ 0.9 means “very high confidence”.

Active Table for the Figure 2

Node 1	Node 2	Node 1 annotation	Node 2 annotation	Confidence score
Mdh2	Cs	Malate dehydrogenase 2	Cytrate synthase	0.996
PDH-A1	DLD	Pyruvate dehydrogenase E1	Dihydrolipoyl dehydrogenase, m	0.991
Acadvl	Hadh	VLC-specific acyl-CoA dehydrogenase	Trifunctional enzyme subunit alpha	0.967
Grpel1	9	GrpE protein homolog 1	Stress-70 protein, mitochondrial	0.964
Acadvl	Cpt2	VLC-specific acyl-CoA dehydrogenase	Carnitine O-palmitoyltransferase 2	0.961
Ivd	Hadh	Isovaleryl-CoA dehydrogenase	Trifunctional enzyme subunit alpha	0.954
Hsd17b10	Hadh	3-hydroxyacyl-CoA dehydrogenase	Trifunctional enzyme subunit alpha	0.931
Mdh2	DLD	Malate dehydrogenase 2	Dihydrolipoyl dehydrogenase	0.89

Hmgcl I79_0153 01	Cs	Hydroxymethylglutaryl-CoA lyase	Cytrate synthase	0.877
Tufm	Hspg2 HSPA 9	Nidogen 1.2 Mitochondrial elongation factor Tu	Heparan sulfate core protein	0.867
Col6a1	Sparc	Collagen alpha-1(VI) chain Mitochondrial elongation factor Tu	Stress-70 protein, mitochondrial Kazal-like domain-containing protein	0.859
Tufm	Mdh2	Serine hydroxymethyltransferase	Malate dehydrogenase 2	0.84
Shmt2	DLD	Mitochondrial elongation factor Tu	Dihydrolipoyl dehydrogenase, m	0.828
Tufm	DLD	Mitochondrial elongation factor Tu	Dihydrolipoyl dehydrogenase, m	0.823
Tufm I79_0153 01	Grpel 1	Mitochondrial elongation factor Tu	GrpE protein homolog 1	0.776
App	Sparc	Nidogen 1.2	Kazal-like domain-containing protein	0.768
Hsp90b1	Clu HSPA 9	Amyloid-beta A4 protein HSP90, beta	Clusterin	0.76
Mdh2	Hmgcl	Malate dehydrogenase 2	Stress-70 protein, mitochondrial Hydroxymethylglutaryl-CoA lyase	0.736
Cpt2	PDH- A1	Carnitine O- palmitoyltransferase 2	Pyruvate dehydrogenase E1, subunit α	0.734
Shmt2	Tufm	Serine hydroxymethyltransferase	Mitochondrial elongation factor Tu	0.711
				0.703
				0.692